Available online at www.sciencedirect.com
SCIENCE DIRECT®
Bioorganic & Medicinal Chemistry Letters 15 (2005) 107–113
Bioorganic & Medicinal Chemistry Letters

Estrogen receptor ligands. Part 9: Dihydrobenzoxathiin SERAMs with alkyl substituted pyrrolidine side chains and linkers

Timothy A. Blizzard,* Frank DiNinno, Jerry D. Morgan, II, Helen Y. Chen, Jane Y. Wu, Seongkon Kim, Wanda Chan, Elizabeth T. Birzin, Yi Tien Yang, Lee-Yuh Pai, Paula M. D. Fitzgerald, Nandini Sharma, Ying Li, Zhoupeng Zhang, Edward C. Hayes, Carolyn A. DaSilva, Wei Tang, Susan P. Rohrer, James M. Schaeffer and Milton L. Hammond

Merck Research Laboratories, RY800-B116, PO Box 2000, Rahway, NJ 07065, USA

Received 2 September 2004; revised 8 October 2004; accepted 8 October 2004
Available online 2 November 2004

Abstract—A series of dihydrobenzoxathiin SERAMs with alkylated pyrrolidine side chains or alkylated linkers was prepared. Minor modifications in the side chain or linker resulted in significant effects on biological activity, especially in uterine tissue.

The clinical significance of the selective estrogen receptor modulators (SERMs) is well documented.[1] Recently, there has been much interest in the development of receptor subtype-selective SERMS.[2] Previous reports from this laboratory have reported the discovery of dihydrobenzoxathiins (e.g., **1**) as a novel class of Selective Estrogen Receptor Alpha Modulators (SERAMs).[3a–e] More recently, we have also described our initial studies on the side chain SAR of **1**, which were aimed at maintaining potency and selectivity while reducing oxidative metabolism of the side chain.[3d,e]

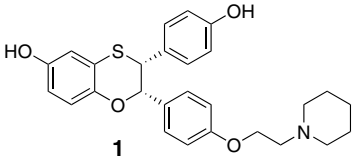

1

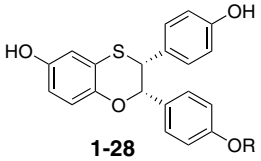

1-28

During the course of these studies, we found that the fused cyclopropyl analog **2** had excellent potency and subtype selectivity while retaining a uterine profile comparable to that of **1** (Table 1). However, like all of the bicyclic analogs that we examined,[3d] **2** appeared to be susceptible to metabolic oxidation of the side chain, as measured by an in vitro liver microsome assay.[4] Interestingly, the unsubstituted pyrrolidine analog **3** did not form a detectable cyanide adduct in this assay. However, **3** had a less favorable SERM profile than **1**, particularly with regard to uterine agonism/antagonism.

We therefore targeted analogs **4**–**16** for synthesis with the hope that we could find a pyrrolidine analog with an improved SERM profile that was less susceptible than **1** to oxidation. The requisite aminoalcohol side chain synthons **4a**–**16a** were prepared by a variety of methods as summarized below (Table 1 and Schemes 1–3).[5]

The first method, illustrated by the preparation of the 3-methyl analog **4a**, involved conversion of a chiral diacid, for example, **29**, to the corresponding imide **45** by sequential reaction with acetyl chloride (to form the anhydride), ethanolamine, and acetic anhydride (Scheme 1). As expected, some epimerization occurred during this sequence; imide **45** was obtained in only 71% ee.[6] For initial evaluation, this enantiomerically impure material was converted to the final product, dihydrobenzoxathiin **4**. However, it was possible to obtain enantiomerically pure **4a** by chiral HPLC separation of the enantiomers of **45**[6] followed by reduction of the

Keywords: SERMs; SERAMs; Estrogen.
* Corresponding author. Tel.: +1 732 594 6212; fax: +1 732 594 9556; e-mail: tim_blizzard@merck.com

0960-894X/$ - see front matter © 2004 Elsevier Ltd. All rights reserved.
doi:10.1016/j.bmcl.2004.10.036

Table 1. Side chain preparation summary and biodata for alkylated pyrrolidine analogs

#	R	ER Binding (IC_{50}, nM)[9]			Cyanide adduct?[4]	MCF-7[10] IC_{50} (nM)	Uterine activity[11]		Side chain	Starting material[5]	Scheme (yield)[5]
		hERα	hERβ	β/α			%Ant.	%Ag.			
1	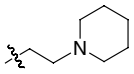	0.8	45	56	Yes	2.8	99	9	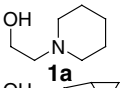 **1a**	Commercial (Aldrich)	
2	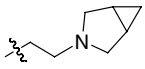	0.7	136	194	Yes	2.6	86	8	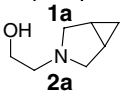 **2a**	See Ref. 4	
3	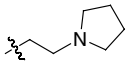	2.6	64	25	No	3.3	72	34	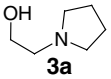 **3a**	Commercial (Aldrich)	
4	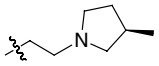	3.0	161	54	No	0.9	106	−19	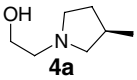 **4a**	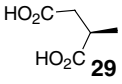 **29**	1 (50)
5	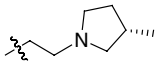	1.0	50	50	No	1.0	85	8	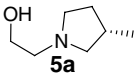 **5a**	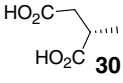 **30**	1 (48)
6	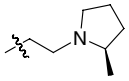	0.7	21	30	No	0.4	83	12	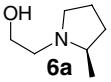 **6a**	 **31**	2 (19)
7	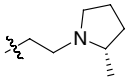	0.8	48	60	No	0.5	22	65	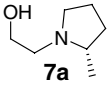 **7a**	**31**	2 (17)
8	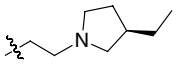	0.9	24	27	—	1.6	31	63	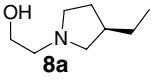 **8a**	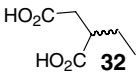 **32**	1 (26)
9	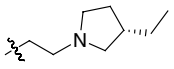	1.1	19	17	—	1.2	14	77	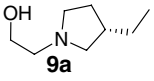 **9a**	**32**	1 (26)
10	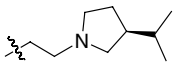	0.4	13	33	Yes	3.5	27	36	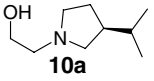 **10a**	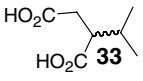 **33**	1 (23)
11	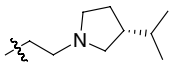	0.3	13	43	Yes	3.8	34	46	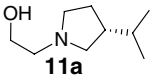 **11a**	**33**	1 (17)
12	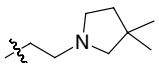	1.0	45	45	Yes	0.7	78	2	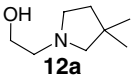 **12a**	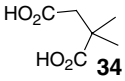 **34**	1 (11)
13	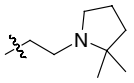	0.9	59	65	Yes	0.4	3	98	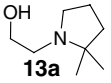 **13a**	 **35**	3 (39)
14	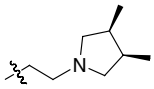	0.7	73	104	No	0.5	75	22	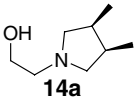 **14a**	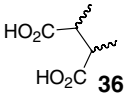 **36**	1 (7)
15	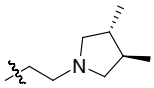	0.5	37	74	Weak	0.4	103	−10	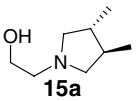 **15a**	**36**	1 (6)
16	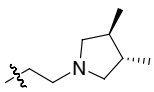	0.4	22	55	No	—	52	39	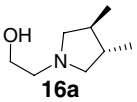 **16a**	**36**	1 (6)
—	Raloxifene	1.8	12	7	No	0.8	81	24	n/a	n/a	n/a
—	17β-Estradiol	1.3	1.1	1	—	—	—	100[11b]	n/a	n/a	n/a

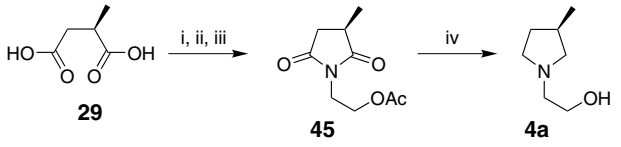

Scheme 1. Reagents and conditions: (i) AcCl (neat), reflux, 3 h; (ii) ethanolamine, Et_3N, CH_2Cl_2, rt, 18 h; (iii) $ClCH_2CH_2Cl$, Ac_2O, reflux, 5 h; (iv) chiral HPLC (see Ref. 6); (v) $LiAlH_4$, ether, 15 h.

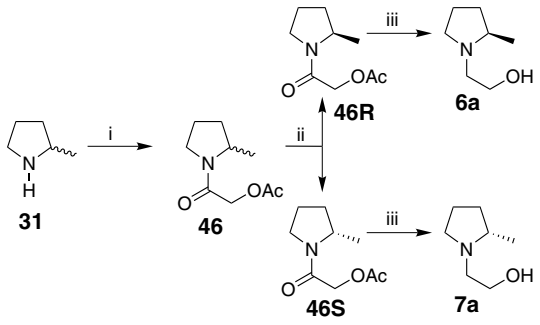

Scheme 2. Reagents and conditions: (i) acetoxyacetyl chloride, Et_3N, CH_2Cl_2; (ii) chiral HPLC; (iii) $LiAlH_4$, Et_2O.

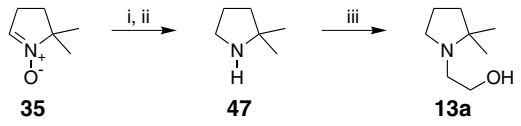

Scheme 3. Reagents and conditions: (i) H_2, Pd/C, EtOH; (ii) 1 N HCl, ether; (iii) 2-bromoethanol, K_2CO_3, MeCN, reflux.

enantiomerically pure imide. Mosher ester analysis of **4a** showed that no epimerization occurred during the imide reduction.[7] Amines **4a**, **5a**, and **12a** were prepared by this route.[5] In a similar approach starting with a racemic diacid, such as **32** or **33**, chiral HPLC separation of the imide provided both side chain enantiomers. Amines **8a**–**11a** were prepared in this manner. Application of a similar sequence to the diastereomeric diacid mixture **36** afforded the 2,3-dimethyl pyrrolidine side chains **14a**–**16a**. Stereochemistry of diasteromers **15** and **16** was established by X-ray analysis of a complex of **15** bound in ERα (vide infra).

The enantiomeric 2-methyl pyrrolidine side chains **6a** and **7a** were prepared by acylation of racemic 2-methyl pyrrolidine **31** followed by chiral HPLC resolution of **46** and reduction of the enantiomeric amides **46*R*** and **46*S*** (Scheme 2).[8]

The 2,2-dimethylpyrrolidine side chain **13a** was prepared by alkylation of 2,2-dimethyl pyrrolidine **47**, which was, in turn, derived from the commercial N-oxide **35** (Scheme 3).

Synthesis of the final products proceeded via attachment of the hydroxyethylamine side chains to the benzoxathiin core (+)-**48** using the previously reported procedure[3a,c] followed by deprotection (Scheme 4).

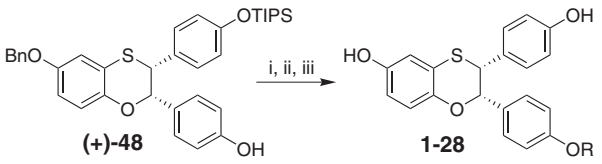

Scheme 4. Reagents and conditions: (i) **1a**–**24a**, DIAD, PPh_3, THF; (ii) Pd, HCO_2NH_4, EtOH, EtOAc, H_2O; (iii) *n*-Bu_4NF, AcOH, THF.

All of the novel alkylated pyrrolidine analogs (**4**–**16**) retained the excellent ERα potency exhibited by the initial analogs **1**–**3** (Table 1) in an in vitro estrogen receptor binding assay.[9] Although the magnitude of receptor subtype selectivity (ERβ/ERα ratio) varied considerably (from 17× to 104×), all of the novel analogs were α selective. In addition, all of the new analogs that were tested in the MCF-7 assay retained excellent potency.[10] As we had hoped, the mono-substituted pyrrolidine analogs more closely resembled the unsubstituted pyrrolidine **3** rather than the fused pyrrolidine **2** in the cyanide adduct assay.[4] Interestingly, there was a clear trend toward increased metabolic activation as the size of the pyrrolidine substituent increased. Fortunately, the smaller substituents, which resulted in improved metabolic stability also conferred an improved uterine profile. In fact, several of the novel analogs exhibited a substantially improved uterine profile relative to the unsubstituted pyrrolidine **3**.[11] The 3-(*R*)-methyl pyrrolidine side chain present in **4** was especially noteworthy in this regard. It is interesting that the uterine profile appears to be highly dependent on the size and stereochemistry of the pyrrolidine ring substituent. Substituents that are larger than methyl are clearly detrimental (compare **4**, **8**, and **10**) and the 3-(*R*) stereochemistry is better than 3-(*S*) (compare **4** and **5**).

Similarly, for the 3,4-dimethyl pyrrolidine analogs **14**–**16**, the 3*R*,4*R* isomer **15** is clearly superior to the other diastereomers **14** and **16**, at least in terms of uterine activity. Another striking stereochemical effect is seen with compounds substituted at C-2 of the pyrrolidine ring. The 2-(*S*) methyl analog **7** has a substantially inferior uterine profile relative to the 2-(*R*) analog **6**. This is also illustrated by the large difference in uterine activity between the 3,3-dimethyl analog **12** (a potent uterine antagonist) and the corresponding 2,2-dimethyl analog **13** (a potent agonist in uterine tissue).

SERM side chains are generally connected to the core structure by an unsubstituted ethylene linker. Encouraged by the superior uterine profiles of the methylated pyrrolidines, we decided to examine methylated linkers to see if a similar improvement in activity could be obtained by adding a methyl group to the linker. To verify that the two carbon linker was optimal we first prepared the three carbon analog **17**. The requisite side chain **17a** was readily prepared from pyrrolidine (Scheme 5) and attached to the dihydrobenzoxathiin core using our standard protocol (Scheme 4). The extended linker was clearly detrimental with regard to uterine activity (Table 2; compare **3** and **17**). The alkylated-linker side chains were easily synthesized by bis-alkylation of the

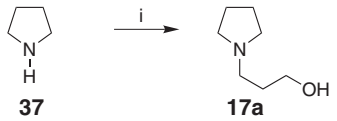

Scheme 5. Reagents and conditions: (i) 3-bromopropanol, K_2CO_3, MeCN, reflux.

appropriate amine precursor with 1,4-dibromobutane. For example, the α-(*S*)-methyl side chain **18a** was prepared from commercial L-alaninol **38** in one step (Scheme 6). Side chains **18a**–**24a** were prepared in this manner.

With the alkylated linker, attachment of the side chain to the dihydrobenzoxathiin core was complicated by the formation of a by-product, such as **25**, which results from the presence of an unsymmetrical intermediate, such as **49**, in the Mitsunobu alkylation (Scheme 7). Reaction of **49** with the phenol of (+)-**48** via 'path a' eventually leads to the 'normal' product **18** while alkylation via 'path b' results in the rearranged by-product

Table 2. Side chain preparation summary and biodata for linker alkylated analogs

#	R	ER Binding (IC_{50}, nM)[9]			Cyanide adduct?[4]	MCF-7[10] IC_{50} (nM)	Uterine activity[11]		Side chain	Starting material[5]	Scheme (yield)[5]
		hERα	hERβ	β/α			%Ant.	%Ag.			
3	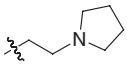	2.6	64	25	No	3.3	72	34	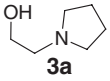 **3a**	Commercial (Aldrich)	
17	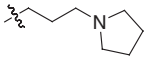	1.7	81	48	—	4.1	26	69	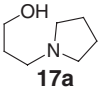 **17a**	 **37**	5 (67)
18	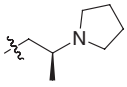	1.3	45	35	No	0.3	101	0	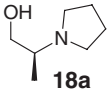 **18a**	 **38**	6 (58)
19	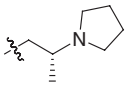	1.7	71	42	Weak	0.5	18	71	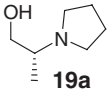 **19a**	 **39**	6 (48)
20	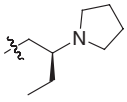	0.5	25	56	Yes	0.2	61	26	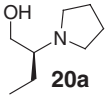 **20a**	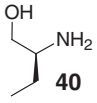 **40**	6 (57)
21	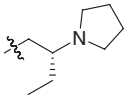	0.7	38	51	Yes	0.4	2	78	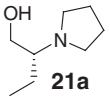 **21a**	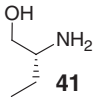 **41**	6 (50)
22	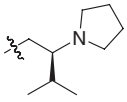	0.7	46	66	Yes	2.0	44	55	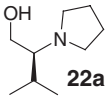 **22a**	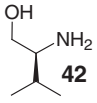 **42**	6 (80)
23	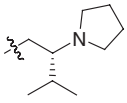	0.5	15	30	Yes	0.4	20	79	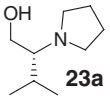 **23a**	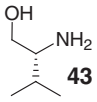 **43**	6 (92)
24	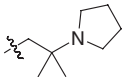	0.7	44	63	No	0.5	31	71	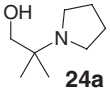 **24a**	 **44**	6 (44)
25	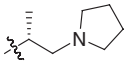	2.5	176	70	—	2.3	68	29	**25** is a by-product from synthesis of **18**		
26	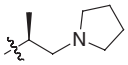	6.3	363	58	—	9.1	21	26	**26** is a by-product from synthesis of **19**		
27	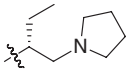	0.8	97	120	Yes	1.3	30	28	**27** is a by-product from synthesis of **20**		
28	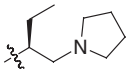	1.2	114	95	Yes	3.1	28	40	**28** is a by-product from synthesis of **21**		
—	Raloxifene	1.8	12	7	No	0.8	81	24	n/a	n/a	n/a
—	17β-Estradiol	1.3	1.1	1	—	—	—	100[11b]	n/a	n/a	n/a

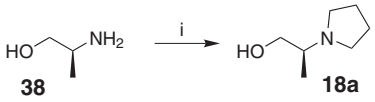

Scheme 6. Reagents and conditions: (i) 1,4-dibromobutane, K_2CO_3, MeCN, reflux.

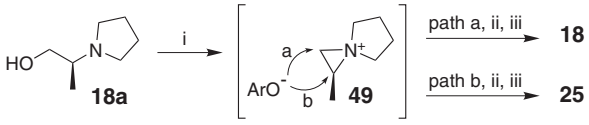

Scheme 7. Reagents and conditions: (i) (+)-**49**, DIAD, PPh_3, THF; (ii) Pd, HCO_2NH_4, EtOH, EtOAc, H_2O; (iii) *n*-Bu_4NF, AcOH, THF.

25. Fortunately, the two products could be separated by chromatography.

The biodata and preparation of the alkylated linker analogs are summarized in Table 2. Introduction of a methyl group at the α position of the ethylene linker did result in an improved SERM profile provided that the new stereocenter had the (*S*) stereochemistry. As with the alkylated pyrrolidines, the size of the substituent had a strong impact on metabolic activation with larger substituents resulting in increased oxidation as measured by cyanide adduct formation. Similarly, uterine activity was highly dependent on the stereochemistry and site of alkylation as well as the size of the substituent. For example, while an (*S*)-methyl substituent at the α position (next to nitrogen) of the linker improved the SERM profile, an (*R*)-methyl at this position resulted in a substantially less favorable profile (compare **18** and **19**). Larger substituents at this position resulted in an increase in uterine agonism. Alkylation at the beta position (next to the oxygen) also resulted in a less desirable uterine profile (compounds **25**–**28**).

X-ray analysis[12] of complexes of **15**, **16**, **18**, and **19** bound to the ligand-binding domain of ERα provides a possible explanation for the extraordinary uterine antagonism of **15** and **18**, and the partial agonism of **16** and **19**. As is illustrated in Figure 1, the disposition of the methyl substituents of **15** allows a close hydrophobic interaction of the pyrrolidine ring with W383, and with L536 and L539, two residues in helix 12. The methyl substituents also allow a close approach of residues C530 and K531, in the loop that connects helix 11–12. We suggest that all of these interactions may serve to stabilize helix 12 in the antagonist conformation, leading to the observed extreme uterine antagonism. In contrast, the downward disposition of the methyl substituent on the right in **16** (Fig. 1) forces the compound to the left (in the view of that figure) to avoid steric clash with W383, generating fewer hydrophobic interactions with W383, L536, and L539. In addition, the upward disposition of the methyl on the left puts steric pressure on K531, forcing it and the entire connecting loop away from the ligand. We suggest that the less favorable interactions in the complex with **16** do not provide added stabilization for helix 12 in the antagonist conformation, explaining the partial agonism of this compound.

There is a caveat to our proposal that the extreme uterine antagonism of **15** is a result of the stabilization of helix 12 in the antagonist conformation via direct interactions with residues in helix 12 as well as stabilizing interactions with residues in the loop that connects helices 11 and 12. We might expect that the residues in the connecting loop (residues 526–532) would be significantly better ordered in **15** than in **16**, but in fact the loop is poorly ordered in both of these complexes. The order is somewhat better for **15** than for **16**, but it is still very poor in absolute terms. We suspect that the poor ordering of the connecting loop is an artifact induced by the fact that the protein was carboxymethylated during the purification process, to prevent aggregation via the formation of interresidue disulfide bonds. C530 is one of the modified residues, and the modification probably prevents the close approach of the connecting loop to the antagonist arm of the ligand. Such density as is observed for this loop is probably due to a subpopulation of unmodified C530 residues. But even without the full ordering of the connecting loop, **15** makes

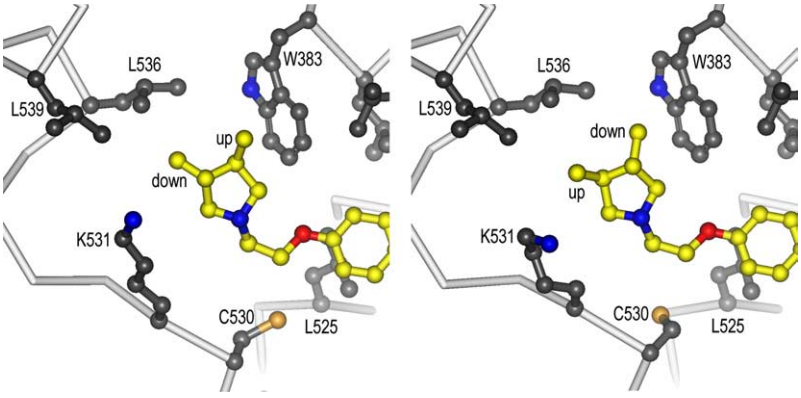

Figure 1. The structures of **15** (left) and **16** (right) bound to the ligand-binding domain of ERα. Nitrogen atoms are colored blue, oxygen red, and sulfur gold. Carbon atoms in the ligand are colored yellow, and carbon atoms in the protein are colored gray. Protein residues that contain at least one atom within 5.0 Å of an atom in the ligand are show (residues in helix 3, which are on top in this view, have been removed for clarity). To emphasize the stereochemistry of the methyl substituents on pyrrolidine ring, the labels 'up' and 'down' have been added.

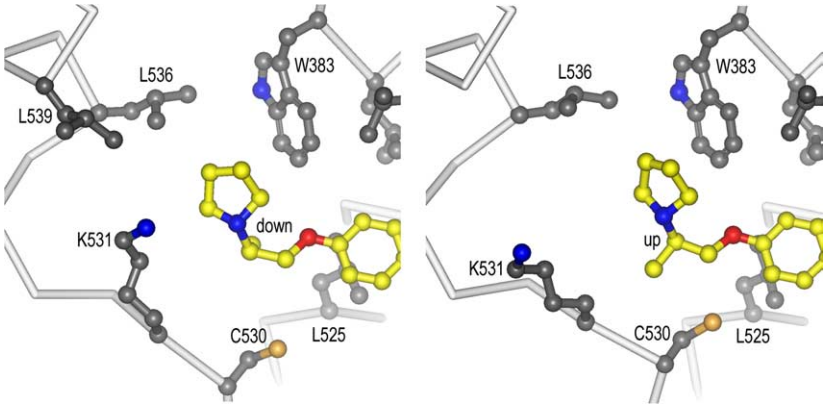

Figure 2. The structures of **18** (left) and **19** (right) bound to the ligand-binding domain of ERα. Atom coloring and residue labeling is as in Figure 1.

significantly better direct contacts with residues in helix 12 than does **16**, supporting our hypothesis.

Further support comes from a second pair of structures, **18** and **19**, where the methyl substituents are now on the linker, not the ring. As is illustrated in Figure 2, the down disposition of the methyl substituent of **18** allows a close approach of the ring to W383, and good interactions with L536 and L539. In the structure of **19**, the up orientation of the methyl group generates a serious steric clash with K531, causing the pyrrolidine ring to twist. This reduces the interaction with W383, and loses the interaction with L539 completely. Once again, **18**, the compound with better interactions with residues in helix 12 and with the connecting loop, is the full antagonist.

In conclusion, we have demonstrated that the SERM profile of the dihydrobenzoxathiin SERAMs is highly dependent on the size and location of side chain substituents. Several of the novel compounds described herein are clearly superior to our starting compound **1**. Compounds **4**, **15**, and **18** are especially noteworthy in this regard. However, believing that further improvement might be possible, we have continued our effort in this area. The result of this ongoing effort will be reported in future publications from this laboratory.

Acknowledgements

The authors thank Dr. Derek Von Langen and Ms. Judy Pisano for the preparation of (+)-**48** and to Dr. Mats Carlquist and his colleagues at Karo-Bio for providing protein samples. Use of the Advanced Photon Source beamline 17-ID was supported by the companies of the Industrial Macromolecular Crystallography Association through a contract with Illinois Institute of Technology.

References and notes

1. (a) Jordan, V. C. *J. Med. Chem.* **2003**, *46*, 883; (b) Jordan, V. C. *J. Med. Chem.* **2003**, *46*, 1081.
2. (a) Malamas, M. S.; Manas, E. S.; McDevitt, R. E.; Gunawan, I.; Xu, Z.; Collini, M. D.; Miller, C. P.; Dinh, T.; Henderson, R. A.; Keith, J. C.; Harris, H. A. *J. Med. Chem.* **2004**, *47*, 5021; (b) Collini, M. D.; Kaufman, D. H.; Manas, E. S.; Harris, H. A.; Henderson, R. A.; Xu, Z. B.; Unwalla, R. J.; Miller, C. P. *Bioorg. Med. Chem. Lett.* **2004**, *14*, 4925; (c) Yang, W.; Wang, Y.; Ma, Z.; Golla, R.; Stouch, T.; Seethala, R.; Johnson, S.; Zhou, R.; Gungor, T.; Feyen, J. H. M.; Dickson, J. K. *Bioorg. Med. Chem. Lett.* **2004**, *14*, 2327; (d) Yang, C.; Edsall, R. J.; Harris, H. A.; Zhang, X.; Manas, E. S.; Mewshaw, R. E. *Bioorg. Med. Chem.* **2004**, *12*, 2553; (e) Chesworth, R.; Zawistoski, M. P.; Lefker, B. A.; Cameron, K. O.; Day, R. F.; Mangano, F. M.; Rosati, R. L.; Colella, S.; Petersen, D. N.; Brault, A.; Lu, B.; Pan, L. C.; Perry, P.; Ng, O.; Castleberry, T. A.; Owen, T. A.; Brown, T. A.; Thompson, D. D.; DaSilva-Jardine, P. *Bioorg. Med. Chem. Lett.* **2004**, *14*, 2729; (f) Meyers, M. J.; Sun, J.; Carlson, K. E.; Marriner, G. A.; Katzenellenbogen, B. S.; Katzenellenbogen, J. A. *J. Med. Chem.* **2001**, *44*, 4230; (g) Mortensen, D. S.; Rodriguez, A. L.; Carlson, K. E.; Sun, J.; Katzenellenbogen, B. S.; Katzenellenbogen, J. A. *J. Med. Chem.* **2001**, *44*, 3838; (h) Muthyala, R. S.; Carlson, K. E.; Katzenellenbogen, J. A. *Bioorg. Med. Chem. Lett.* **2003**, *13*, 4485; (i) Henke, B. R.; Consler, T. G.; Go, N.; Hale, R. L.; Hohman, D. R.; Jones, S. A.; Lu, A. T.; Moore, L. B.; Moore, J. T.; Orband-Miller, L. A.; Robinett, R. G.; Shearin, J.; Spearing, P. K.; Stewart, E. L.; Turnbull, P. S.; Weaver, S. L.; Williams, S. P.; Wisely, G. B.; Lambert, M. H. *J. Med. Chem.* **2002**, *45*, 5492; (j) Schopfer, U.; Schoefter, P.; Bischoff, S. F.; Nozulak, J.; Feuerbach, D.; Floersheim, P. *J. Med. Chem.* **2002**, *45*, 1399.
3. (a) Kim, S.; Wu, J. Y.; Birzin, E. T.; Frisch, K.; Chan, W.; Pai, L.; Yang, Y. T.; Mosley, R. T.; Fitzgerald, P. M. D.; Sharma, N.; DiNinno, F.; Rohrer, S.; Schaeffer, J. M.; Hammond, M. L. *J. Med. Chem.* **2004**, *47*, 2171; (b) Chen, H. Y.; Kim, S.; Wu, J. Y.; Birzin, E. T.; Chan, W.; Yang, Y. T.; DiNinno, F.; Rohrer, S.; Schaeffer, J. M.; Hammond, M. L. *Bioorg. Med. Chem. Lett.* **2004**, *14*, 2551; (c) Kim, S.; Wu, J.; Chen, H. Y.; Birzin, E. T.; Chan, W.; Yang, Y. T.; Colwell, L.; Li, S.; DiNinno, F.; Rohrer, S.; Schaeffer, J. M.; Hammond, M. L. *Bioorg. Med. Chem. Lett.* **2004**, *14*, 2741; (d) Blizzard, T. A.; DiNinno, F.; Morgan, J. D., II; Chen, H. Y.; Wu, J. Y.; Gude, C.; Kim, S.; Chan, W.; Birzin, E. T.; Yang, Y.; Pai, L.; Zhang, Z.; Hayes, E. C.; DaSilva, C. A.; Tang, W.; Rohrer, S. P.; Schaeffer, J. M.; Hammond, M. L. *Bioorg. Med. Chem. Lett.* **2004**, *14*, 3861; (e) Blizzard, T. A.; DiNinno, F.; Morgan, J. D., II; Wu, J. Y.; Chen, H. Y.; Kim, S.; Chan, W.; Birzin, E. T.; Yang, Y.; Pai, L.; Zhang, Z.; Hayes, E. C.; DaSilva, C. A.; Tang, W.; Rohrer, S. P.; Schaeffer, J.

M.; Hammond, M. L. *Bioorg. Med. Chem. Lett.* **2004**, *14*, 3865.

4. Compounds were incubated with liver microsomes in the presence of cyanide ion then LC–MS was used to analyze for the presence of cyanide adducts. This cyanide adduct assay was used as a surrogate measure of protein adduct formation subsequent to microsomal oxidation. For more details, see (a) Evans, D. C.; Watt, A. P.; Nicoll-Griffith, D. A.; Baillie, T. A. *Chem. Res. Toxicol.* **2004**, *17*, 3.
5. All new compounds were characterized by LC–MS and 400, 500, or 600 MHz ^{1}H NMR. Side chains were prepared using starting materials and methods indicated in Tables 1 and 2 (yields are the overall yield of the side chain from the indicated starting material). Starting material sources: **29**–**31** and **34**–**44**: Aldrich; **32** and **33** were prepared from the corresponding alkyl diethylmalonates (Aldrich) by a procedure analogous to a literature synthesis of 2,3-dimethyl succinic acid: Sutton, S. C.; Nantz, M. H.; Hitchcock, S. R. *Org. Prep. Proc. Int.* **1992**, *24*, 39.
6. Enantiomeric excess of **45** was determined by chiral HPLC analysis on a Chiralcel OD 4.6 × 250 mm 10 μm column eluted with 4:1 heptane–isopropanol at 0.4 mL/min. Under these conditions, the (*R*)-enantiomer of **45** has a retention time of 31.8 min while the (*S*)-enantiomer elutes at 36.2 min.
7. Enantiomeric purity of **4a** was confirmed by analysis of the 600 MHz ^{1}H NMR of the Mosher ester of **4a**. The Mosher ester of racemic **4a** was also prepared for comparison.
8. The stereochemistry assignments of **6a** and **7a** were made by comparison of their optical rotations to an authentic sample of the (*S*)-enantiomer **7a**, which was prepared from the known (*S*)-*N*-benzoyl-2-methyl-pyrrolidine: (a) Ringdahl, B. *Acta Chem. Scand. Ser. B* **1984**, *38*, 141.
9. The IC_{50} values were generated in an estrogen receptor ligand binding assay. This scintillation proximity assay was conducted in NEN Basic Flashplates using tritiated estradiol and full length recombinant human ERα and ERβ proteins. Compounds were evaluated in duplicate in a single assay. In our experience, this assay provided IC_{50} values that are reproducible to within a factor of 2–3. Benzoxathiin **1** ($n = 36$) and estradiol ($n > 100$) were tested in multiple assays; data reported in Table 1 are an average of all determinations.
10. An in vitro MCF-7 breast cancer cell proliferation assay adapted to a 96-well format. Cells were grown in estrogen-depleted media for 6 days then treated with the test compound for 7 days. To evaluate the antagonist activity of a test compound, this treatment occurs in the presence of low levels of estradiol. The protein content of living cells is then measured and an IC_{50} determined.
11. (a) The uterine weight assay is an in vivo assay that measures estrogen agonism and antagonism in rat uterine tissue. Compounds are dosed orally at 1 mpk. Agonism is reported as % of estradiol control; antagonism reported as %antagonism of estradiol; (b) Estradiol exhibited 100% agonism at 4 μg/kg.
12. Complexes of the ligand binding domain of ERα (residues 307–554) with the ligands **15**, **16**, **18**, and **19** were crystallized by vapor diffusion, using a precipitant containing 100 mM $MgCl_2$, 6% PEG 3350, and 100 mM imidazole buffer, pH 7.1. The space group of the crystals was $P6_522$, with cell dimensions $a = b = 58.62$, $c = 276.79$ (**15**), $a = b = 58.57$, $c = 276.31$ (**16**), $a = b = 58.64$, $c = 275.77$ (**18**), and $a = b = 58.69$, $c = 277.18$ (**19**). Diffraction data for all complexes were measured at beamline 17-ID of the Advanced Photon Source. The data were processed with program X-GEN, which yielded an R-merge of 0.073 for the data from ∞ to 1.8 Å (**15**), 0.060 for the data from ∞ to 1.7 Å (**16**), 0.083 for the data from ∞ to 1.8 Å (**18**), and 0.066 for the data from ∞ to 1.6 Å (**19**). The structures were refined using program SHELXL, with final values for R-work and R-free of 0.181 and 0.269 for the data from 10.0 to 1.80 Å resolution (**15**), 0.177 and 0.267 for the data from 10.0 to 1.70 Å (**16**), 0.187 and 0.299 for the data from 10.0 to 1.80 Å (**18**), and 0.184 and 0.251 for the data from 10.0 to 1.60 Å (**19**). Coordinates and structures factors have been deposited with the Protein Data Bank (entries 1XP1, 1XP6, 1XP9, and 1XPC).